

Highly conductive indium nanowires deposited on silicon by dip-pen nanolithography

Anton Kozhukhov, Anatoliy Klimenko, Dmitriy Shcheglov, Vladimir Volodin, Natalya Karnaeva, and Alexander Latyshev

Citation: *Journal of Applied Physics* **117**, 145305 (2015); doi: 10.1063/1.4917530

View online: <http://dx.doi.org/10.1063/1.4917530>

View Table of Contents: <http://scitation.aip.org/content/aip/journal/jap/117/14?ver=pdfcov>

Published by the **AIP Publishing**

Articles you may be interested in

[Mechanism of force mode dip-pen nanolithography](#)

J. Appl. Phys. **115**, 174314 (2014); 10.1063/1.4875665

[Electrical conductivity of ultra-thin silicon nanowires](#)

J. Vac. Sci. Technol. B **26**, 159 (2008); 10.1116/1.2823056

[Capturing and depositing one nanoobject at a time: Single particle dip-pen nanolithography](#)

Appl. Phys. Lett. **90**, 133102 (2007); 10.1063/1.2714287

[Direct deposition of continuous metal nanostructures by thermal dip-pen nanolithography](#)

Appl. Phys. Lett. **88**, 033104 (2006); 10.1063/1.2164394

[Conductivity-based contact sensing for probe arrays in dip-pen nanolithography](#)

Appl. Phys. Lett. **83**, 581 (2003); 10.1063/1.1592620



You don't still use this cell phone

or this computer

Why are you still using an AFM designed in the 80's?

It is time to upgrade your AFM

Minimum \$20,000 trade-in discount for purchases before August 31st

Asylum Research is today's technology leader in AFM

dropmyoldAFM@oxinst.com

OXFORD
INSTRUMENTS
The Business of Science®

Highly conductive indium nanowires deposited on silicon by dip-pen nanolithography

Anton Kozhukhov,^{1,2} Anatoliy Klimenko,¹ Dmitriy Shcheglov,¹ Vladimir Volodin,^{1,2} Natalya Karneeva,¹ and Alexander Latyshev¹

¹*Rzhanov Institute of Semiconductor Physics, Siberian Branch of Russian Academy of Sciences, Novosibirsk 630090, Russia*

²*Novosibirsk State University, Novosibirsk 630090, Russia*

(Received 7 October 2014; accepted 2 April 2015; published online 13 April 2015)

In this paper, we developed a new dip-pen nanolithography (DPN) method. Using this method, we fabricated conductive nanowires with diameters of 30–50 nm on silicon substrates. To accomplish this, indium was transferred from an atomic force microscopy tip to the surface by applying a potential difference between the tip and substrate. The fabricated indium nanowires were several micrometers in length. Unlike thermal DPN, our DPN method hardly oxidized the indium, producing nanowires with conductivities from 5.7×10^{-3} to $4 \times 10^{-2} \Omega \text{ cm}$. © 2015 Author(s). All article content, except where otherwise noted, is licensed under a Creative Commons Attribution 3.0 Unported License. [<http://dx.doi.org/10.1063/1.4917530>]

I. INTRODUCTION

Dip-pen nanolithography (DPN)^{1,2} is a method by which metals or organic compounds can be directly deposited on a substrate from an atomic force microscopy (AFM) tip. This technique is useful in nanoelectronics as a way to fabricate conducting nanowires^{3,4} and in studying biomolecules and polymers in controlled locations.^{5–7} DPN can produce conducting structures with resolution better than 50 nm on a semiconductor surface.^{8,9} In thermal DPN, metal is transferred from an AFM probe onto the surface by heating the probe to the melting point of the loaded metal.³ Metals with low melting points such as indium, tin, and lead are required. When the metal on the probe tip is heated to its melting point, it transfers to the surface of the semiconductor by a metal–surface adhesion force.⁵ However, heating the metal oxidizes it, significantly reducing the conductivity of the fabricated nanostructures.³ To reduce oxidation, in this paper, we deposited metal from an AFM probe by applying an electric potential between the tip and substrate.

II. MATERIALS AND METHODS

Indium (99.99%) was loaded onto the AFM probe tip by thermal vacuum spraying. To control the indium thickness, thermal spraying was performed through a mask with a hole of 6 μm diameter located 2 μm from the probe tip (Fig. 1(b)). To improve adhesion of indium to the probe, a layer of Ni and 30 nm of Cr were first deposited on the probe. Then, indium was deposited with a thickness from 80 to 200 nm (Figs. 1(a) and 1(c)). Indium was deposited from the AFM tip onto the stepped surface of Si (111) with an interaction force of 10^{-7} N between the probe and the surface at room temperature.¹⁰ We fabricated structures with a vertical resolution of 0.2 nm on the smooth surface of Si (111) covered with 15 nm of anodic oxide as an isolation layer, matching our earlier study of local anodic oxidation caused by AFM.¹¹ A positive potential of 10 V was applied to the AFM cantilever (Fig. 2), during

which the indium-coated probe was moved parallel to the surface in lines for 1–2 μm at 0.1 $\mu\text{m/s}$.

III. RESULTS AND DISCUSSION

A. Nanowire formation

Using the indium-coated AFM tip, we fabricated several indium nanowires on the stepped surface of Si(111). The interaction force between the tip and sample and the speed of tip offset were 10^{-7} N and 0.1 $\mu\text{m/s}$, respectively. After fabricating the nanowires, we investigated a section of each sample using AFM, which had a sharp tip with the radius of curvature of less than 10 nm. Figure 3(a) shows an AFM image of indium nanowires on the Si(111) surface. Analyzing the relief profile of the fabricated nanowires, we found their width to be 50–70 nm and their height to be 0.8–1 nm.

To understand how the potential difference and interaction force between the tip and sample influenced the geometries of the indium nanowires, we fabricated several nanowires. In this experiment, the potential difference was varied from 3 to 10 V, and the interaction force was either 10^{-7} N or 5×10^{-6} N. All other parameters were constant. Figure 4 shows the nanowire height as a function of tip potential and of interaction force.

The nanowire diameter depended on both interaction force and tip potential. We propose that indium transferred from the AFM tip to the Si surface through local heating of indium on the tip, caused by the current through the thin layer of indium, which then deposited on the surface through the contact force.

B. Nanowire electrical resistivity

To test the electrical properties of the indium nanowires, we fabricated two isolated Au contacts, separated by 0.3–0.4 μm , each with a thickness of 10 nm, on a dielectric substrate by thermal vacuum deposition through a mask. We



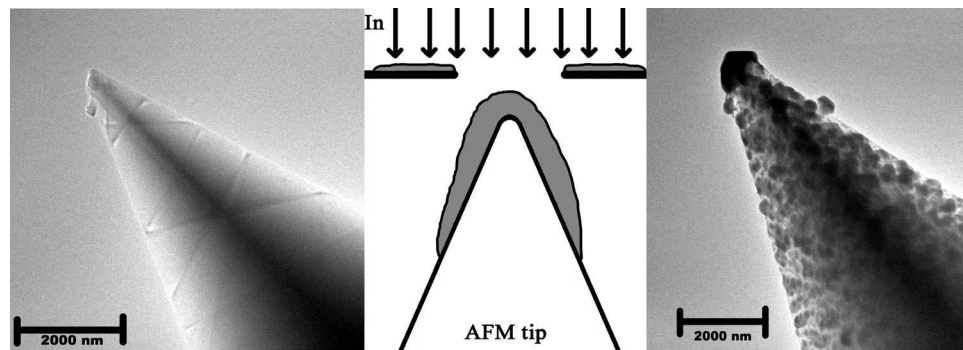


FIG. 1. (a) Transmission electron microscopy (TEM) image of the AFM tip before indium spraying, (b) schematic of indium deposited on the AFM probe tip, and (c) TEM image of the AFM tip after vacuum deposition of indium (thickness of 120 nm).

connected the isolated contacts with either indium or an indium nanowire, then we measured the electrical resistivity between the Au contacts, which also measured the indium conductivity (Figs. 5 and 6). Figure 5 shows AFM images of the contacts before and after connecting them with indium. For this experiment, the potential difference was 25 V and consequently the deposited indium had a height of 400 nm. By applying such a high potential, all the indium on the AFM tip was deposited. The measured electrical resistivity of the indium was $5.7 \times 10^{-3} \Omega \text{ cm}$. Figure 6(a) shows an AFM image of a nanowire with a height of 10 nm. In this experiment, the potential difference was 10 V. The electrical resistivity of this indium nanowire was $4 \times 10^{-2} \Omega \text{ cm}$. We believe the electrical resistivity of the indium (400 nm) was lower than that of the indium nanowire (10 nm) because the former was less oxidized than the latter.

C. Raman scattering spectroscopy

We also studied the samples using Raman scattering spectroscopy (T64000, Horiba Jobin Yvon, France) in the backscattering geometry. The Raman spectrometer was used in a micro-Raman setup, based on an optical microscope (Olympus), equipped with a liquid nitrogen-cooled CCD matrix detector. The sample was excited by the 514.05-nm line of an Ar^+ laser. The spectral resolution was better than 1.5 cm^{-1} . The laser radiation did not significantly heat the samples because the laser power reaching the sample was 1 mW and because the diameter of the laser beam on the sample was $\sim 5 \mu\text{m}$.

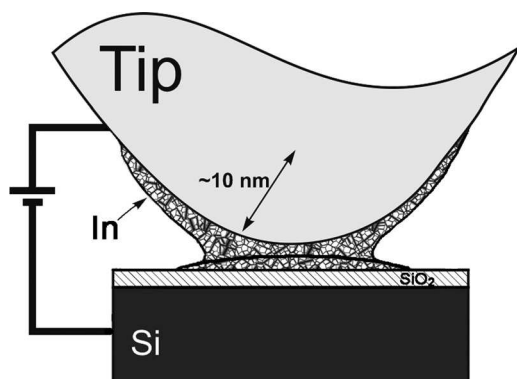


FIG. 2. Schematic of indium deposition from the AFM probe to the substrate while moving the probe along the substrate surface.

Figure 7 shows the Raman spectra of the sample at various locations. Because the indium nanowires were semi-transparent, we could observe the Raman signal from the Si substrate in the studied spectral region. Figure 8 shows spectra of Si (curve 1) and the sample in an area without indium

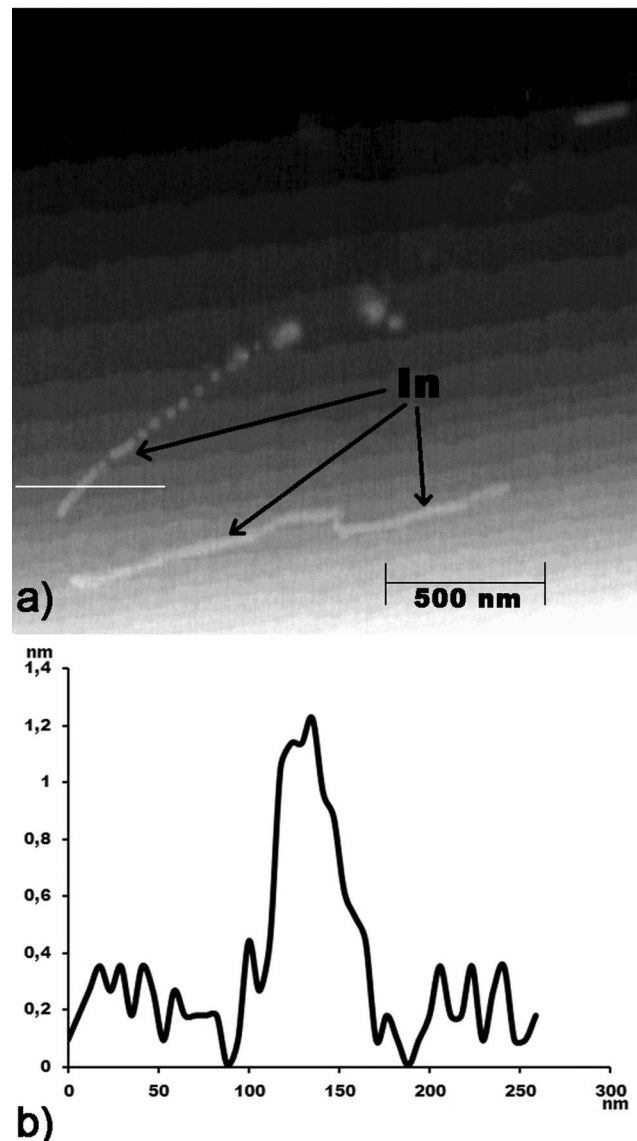


FIG. 3. (a) AFM topographic image of indium nanowires formed on the Si surface, (b) relief profile along the line shown in (a).

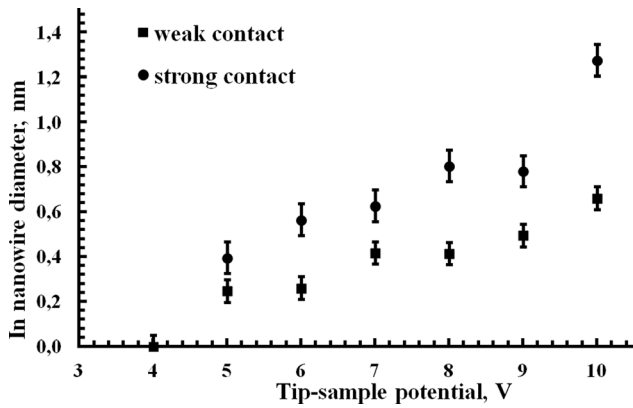


FIG. 4. Indium nanowire diameter as a function of tip potential at weak (10^{-7} N) and strong ($5 \cdot 10^{-6}$ N) contact interaction forces.

(curve 2). There are peculiarities in the Raman spectra caused by two-acoustic-phonon scattering in the Si substrate. The peak at 305 cm^{-1} is caused by 2-TA scattering, and the peak at $420\text{--}430 \text{ cm}^{-1}$ is caused by TA-LA scattering.^{10–12} In a two-phonon scattering process, the quasi-impulse of phonons is not conserved; therefore, because of acoustic phonon dispersion, it appears as modes caused by two-phonon Raman scattering in the Si substrate at $225\text{--}450 \text{ cm}^{-1}$.

A very intense peak from one-phonon scattering at 520 cm^{-1} is not shown here, but the intensity of this peak for curves 2 and 3 is lower than for pure Si (curve 1); therefore, we conclude that the indium coverage absorbs light. At a location with indium (curve 3), the spectrum has a broad peak at $\sim 260 \text{ cm}^{-1}$. According to the RRUFF Raman database (<http://rruff.info/>), this peak can be from indium (270 cm^{-1}). However, our peak is broad and slightly shifted,

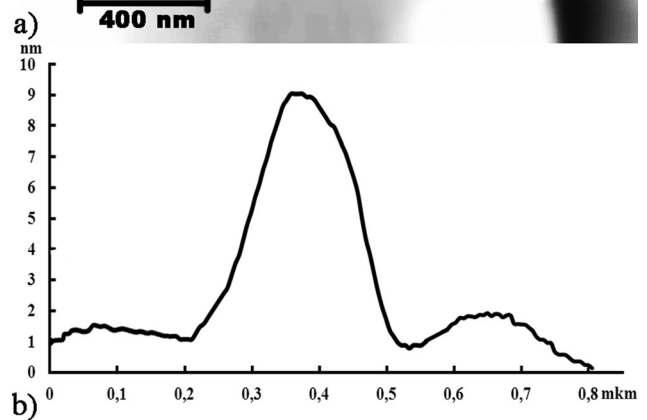
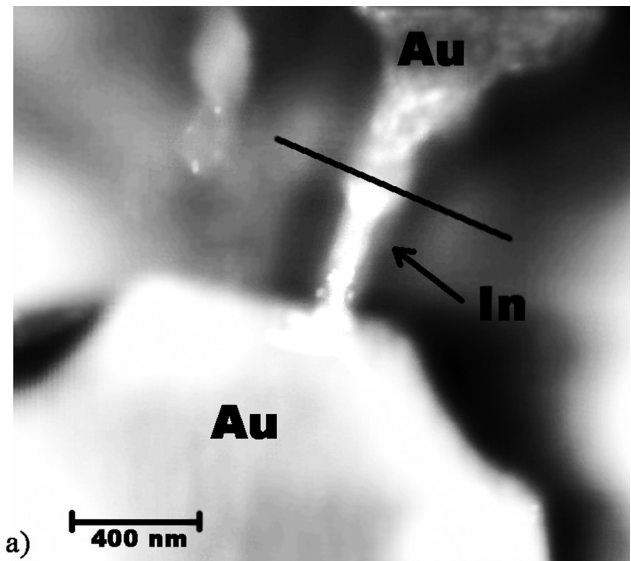


FIG. 6. (a) AFM image of area with connected contacts, (b) relief profile along the line shown in (a).

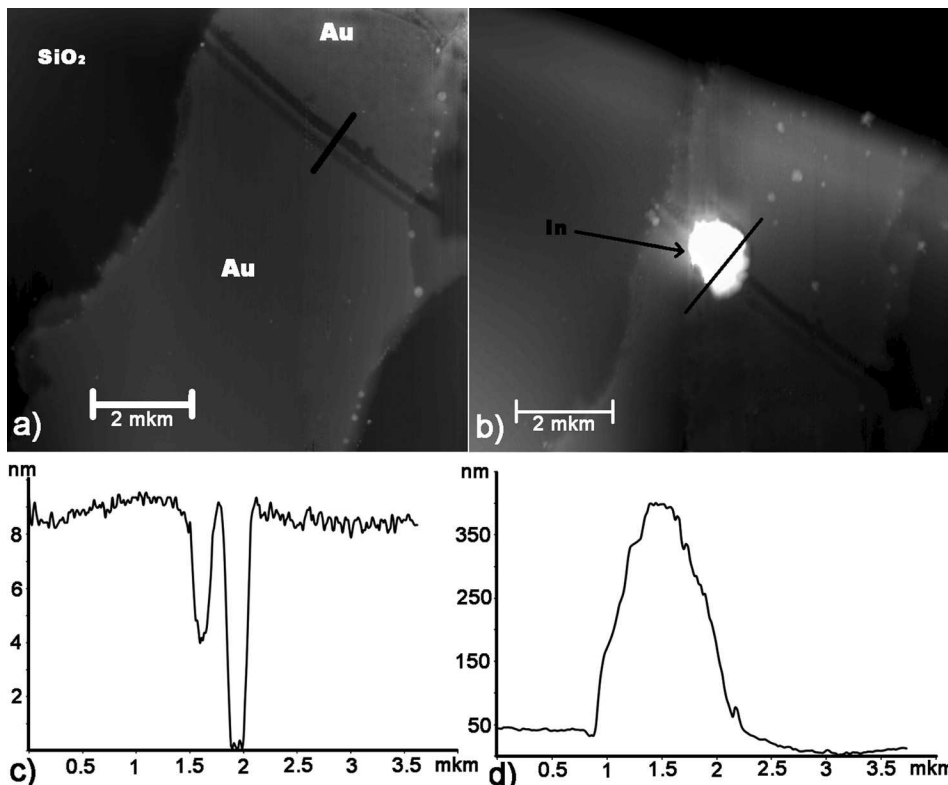


FIG. 5. (a) AFM image of Si surface with Au contacts before indium deposition, (b) AFM image of Si surface with Au contacts after indium deposition, (c) relief profile along the line shown in (a), and (d) relief profile along the line shown in (b).

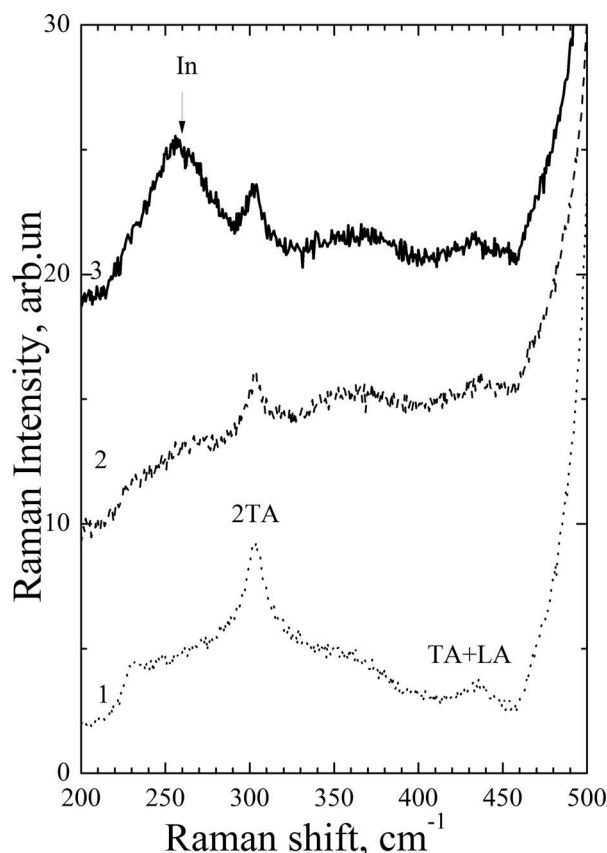


FIG. 7. Raman spectra taken at nanowire (curve 3) and Si substrate (curve 2). Spectrum (1) was taken from pure bulk Si.

so the indium appears amorphous. No peaks related to scattering by indium oxide were detected. One peak did appear related to indium oxide ($\sim 305 \text{ cm}^{-1}$),¹³ which could have been overshadowed by the 2-TA peak from the Si substrate. In any case, if our sample contained indium oxide, it was not sufficiently thick to be detected by Raman scattering here.

IV. CONCLUSION

In summary, we developed a new DPN technique that allows one to fabricate indium nanowires with diameters of 30–50 nm on semiconductors and insulators. Unlike thermal DPN, our DPN technique does not require the AFM tip to be heated to indium's melting point. Indium transport

was possible because of local heating generated by electrical current from the AFM probe tip to the surface under positive potential. The main advantage of this technique is the high conductivity of the produced indium nanowires because of decreased indium oxidation. The measured indium electrical resistivity varied from 5.7×10^{-3} to $4 \times 10^{-2} \Omega \text{ cm}$.

ACKNOWLEDGMENTS

This work was supported by the Russian Foundation for Basic Research (Grant No. 14-02-31032) and the Ministry of Education and Science of the Russian Federation. All experiments were performed using the equipment of CCP "Nanostructures."

¹B. A. Nelson, W. P. King, A. R. Laracuate, P. E. Sheehan, and L. J. Whitman, "Direct deposition of continuous metal nanostructures by thermal dip-pen Nanolithography," *Appl. Phys. Lett.* **88**, 033104 (2006).

²W. M. Wang, M. C. LeMieux, S. Selvarasah, M. R. Dokmeci, and Z. Bao, "Dip-pen nanolithography of electrical contacts to single-walled carbon nanotubes," *ACS Nano* **3**(11), 3543–3551 (2009).

³W.-K. Lee, M. Yang, A. R. Laracuate, W. P. King, L. J. Whitman, and P. E. Sheehan, "Direct-write polymer nanolithography in ultra-high vacuum," *Beilstein J. Nanotechnol.* **3**, 52–56 (2012).

⁴H. Z. Jiang and S. I. Stupp, "Dip-pen patterning and surface assembly of peptide amphiphiles," *Langmuir* **21**, 5242–5246 (2005).

⁵J. H. Lim *et al.*, "Direct-write dip-pen nanolithography of proteins on modified silicon oxide surfaces," *Angew. Chem. Int. Edn.* **42**, 2309–2312 (2003).

⁶B. L. Weeks, A. Noy, A. E. Miller, and J. J. De Yoreo, "Effect of dissolution kinetics on feature size in dip-pen nanolithography," *Phys. Rev. Lett.* **88**, 255505 (2002).

⁷D. Bullen and C. Liu, "Electrostatically actuated dip pen nanolithography probe arrays," *Sens. Actuators A* **125**, 504–511 (2006).

⁸A. V. Latyshev, L. V. Litvin, and A. L. Aseev, "Peculiarities of step bunching on Si(001) surface induced by DC heating," *Appl. Surf. Sci.* **130–132**, 139–145 (1998).

⁹D. V. Sheglov, A. V. Prozorov *et al.*, "Physics of low-dimensional structures," *5/6*, 239–246 (2002).

¹⁰A. V. Kolobov, *J. Appl. Phys.* **87**, 2926 (2000).

¹¹V. A. Volodin, T. T. Korchagina, J. Koch, and B. N. Chichkov, "Femtosecond laser induced formation of Si nanocrystals and amorphous Si clusters in silicon-rich nitride films," *Physica E* **42**(6), 1820–1823 (2010).

¹²V. A. Volodin, D. V. Marin, H. Rinnert, and M. Vergnat, "Formation of Ge and GeSi nanocrystals in $\text{GeO}_x/\text{SiO}_2$ multilayers," *J. Phys. D: Appl. Phys.* **46**, 275305 (7pp) (2013).

¹³D. Liu, W. W. Lei, B. Zou, S. D. Yu, J. Hao, K. Wang, B. B. Liu, Q. L. Cui, and G. T. Zou, "High-pressure x-ray diffraction and Raman spectra study of indium oxide," *J. Appl. Phys.* **104**, 083506 (2008).